Answers to the referees on the article "In-situ airborne measurements of atmospheric and sea surface parameters related to offshore wind parks in the German Bight"

Astrid Lampert[1], Konrad Bärfuss[1], Andreas Platis[2], Simon Siedersleben[3], Bughsin Djath[4],
Beatriz Cañadillas[5], Robert Hunger[1], Rudolf Hankers[1], Mark Bitter[1], Thomas Feuerle[1], Helmut Schulz[1],
Thomas Rausch[1], Maik Angermann[1], Alexander Schwithal[1], Jens Bange[2],
Johannes Schulz-Stellenfleth[4], Thomas Neumann[5], and Stefan Emeis[3]

[1]Institute of Flight Guidance, Technische Universität Braunschweig, Braunschweig, Germany
[2]Eberhard Karls University, Tübingen, Germany
[3]Karlsruhe Institute of Technology, Garmisch-Partenkirchen, Germany
[4]Helmholtz Center for Material and Coastal Research, Geesthacht, Germany
[5]UL International, Oldenburg, Germany

Correspondence: Astrid Lampert (Astrid.Lampert@tu-braunschweig.de)

1 Answers to referee 1

Dear Editor and Reviewers,

We thank you for your kind comments and for taking the time to consider our submitted manuscript. We have incorporated your advice into the revised manuscript that will be resubmitted. Below you will find our direct responses to the comments in

5 normal letters. The comments are given in italic. Our changes to the text are additionally presented in quotation marks.

This paper provides a description of a relatively unique and comprehensive dataset collected using an aircraft platform that contains measurements to evaluate the impact of offshore wind turbines on atmospheric properties. I believe that the paper is very appropriate for ESSD and that the material, in general, is well described. I did have several comments on the material in

10 *the paper that may help to improve the usefulness of the paper to readers outside of the team that collected these measurements. These are included below.*

The authors would like to thank the referee for this positive overall judgement.

Specific Comments:

15 *- Line 74: In the conversion to static temperature, are the pressure and temperature measurements co-located? It may be helpful to have some photographs or diagrams of the payload configuration on the aircraft to better understand how everything is laid out.*

We added a figue showing the nose boom with the sensors and added in the text: "the central sensor package is contained in

the nose boom (Fig. 1)."

20

- Line 102: How does this 1.2 K uncertainty vary with temperature? How linear is this relationship? Is the 20 C value listed the instrument temperature, the air temperature or the surface temperature? Also, what impact does the vertical structure of temperature between the sensor and surface have on the quality of the measurement?

We changed the text to: " It has an accuracy of $\pm 1.2\,\text{K}$ at $20°\,\text{C}$ surface temperature and a temporal resolution of $20\,\text{Hz}$. If no
25 clouds are between the sensor and the surface, the surface temperature measurements are not influenced by the atmospheric temperature or humidity distribution."

- Line 107: Significantly more information could be provided on how surface deflection is calculated using aircraft attitude corrections.

30 We added in the text: "From the point measurements in the scanner's coordinate system $\begin{pmatrix} v_{x_{body}} \\ v_{y_{body}} \\ v_{z_{body}} \end{pmatrix}$, aircraft attitude corrections

using Eulerian angles Ψ, Θ, Φ are applied to rotate aircraft body fixed coordinates into the geodetic coordinate system (positive

directions East, North, Up), which then are geolocated by applying the aircraft position $\begin{pmatrix} p_{x_{body}} \\ p_{y_{body}} \\ p_{z_{body}} \end{pmatrix}$ in the following manner:

$$\begin{pmatrix} p_{x_{geo}} \\ p_{y_{geo}} \\ p_{z_{geo}} \end{pmatrix} = R_{geo}^{body}(-\Psi, -\Theta, -\Phi) \begin{pmatrix} v_{x_{body}} \\ v_{y_{body}} \\ v_{z_{body}} \end{pmatrix} + \begin{pmatrix} p_{x_{body}} \\ p_{y_{body}} \\ p_{z_{body}} \end{pmatrix} \tag{1}$$

Subsequently, the surface deflection η is calculated out of the georeferenced point cloud using mean sea level."

35

- Lines 120-126: Given that the camera images are not publicly available and that they are not included with the main dataset described here, does it make sense to provide more than one sentence on them? I'm not sure that the current configuration aligns with ESSD policies about data availability (not that I disagree with not making the imagery public).

The authors would like to present the whole measurement system of the campaign. If the information about the camera images
40 is not available in the text, the readers will not know about these additional data. So we would like to leave the section in the text, together with the information in the data availability section.

- Lines 128-137: It would be very useful to show some statistics on the regions sampled (e.g. distributions of flight altitudes, distributions of distance from a known shore point, distributions of distance from known wind-farm points).

45 We added a column with the main flight altitude in the tables. See Fig. 4 for an example showing the altitude distribution along the flight path. We think that the map is the most useful illustration of the locations of the flight.

- Figure 2: What are the flight tracks that end abruptly at the coastline? There are several clusters that clearly are going into/out of an airport, but then there are also several singular lines that don't seem to go anywhere.

We added in the figure caption: "Flight tracks end when the data acquisition was shut down."

- Lines 130-131: It might be useful to show a wind rose with these directions on one or both of the maps.

We think that the wind rose is too much information for the map. Anyway measurements were not restricted to the indicated wind directions. This was the general idea, but we have several examples (e.g. Flight 5) where we chose the wind park differently due to other reasons (different flight pattern, etc.). We changed the text to: "Generally, flights were performed downwind of Amrumbank West for a wind direction sector of 80° to 200°, and downwind of Godewind for a sector from 160° to 350°. However, there are exceptions for particular reasons (e.g. during Flight 5 for consecutively probing the wakes of both wind parks, Flight 6 for investigating the changes of the wind field above the wind park)."

It may also be useful to show the extent of German-controlled airspace.

Konrad, is this possible without too much effort? Or should we try to discuss this point?

- Section 4.2: Without going into evaluation/analysis of the data, it might be useful to show an example dataset from one of these CROSS flights. One figure that illustrates the flight pattern followed and some of the structure that might be observed in the key quantities measured might be insightful for the reader.

We added references for each flight pattern in the sections. Further, we added an example of the coastal effect.

- Section 5: For all of these quantities, it might be interesting to pick a few altitudes (e.g. 100, 200, 500 m) and come up with distributions of the mean quantities at these altitudes to plot. This will provide insight into the heterogeneity of the conditions sampled (or lack thereof). One could also imagine looking at scatter plots comparing these mean values (e.g. mean 50 m temperature vs. stability or similar).

According to the analysis shown in other publications based on the data set (Platis et al., 2018; Siedersleben et al., 2018a, b; Platis et al., 2019a; Cañadillas et al., 2019; Siedersleben et al., 2019), the parameters strongly depend on each other. E.g. stable conditions are associated with flow from land if the land surface is warmer than the sea surface. Therefore, we think that scatter plots and statistics that are not taking into account the meteorological situation will not be useful for further analyses.

As an example, instead of showing the mean temperature profile and the range of values around that mean, perhaps it would be insightful to include the distribution of some "stability statistic" (e.g. LTS, etc.). Also, while the mean profiles are interesting, maybe it would also be interesting to show a time-height plot of all of these profiles to demonstrate when the flights took place and whether there were clusters of flights that had similar conditions.

The interaction of the atmospheric boundary layer with wind parks and coastal effects is very complex, and scatter plots or time series alone do not take into account the interactions. Results of detailed scientific analyses can be found in Platis et al.

(2018); Siedersleben et al. (2018a, b); Platis et al. (2019a); Cañadillas et al. (2019); Siedersleben et al. (2019). As an example, we now include Fig. 2, which shows the development of the wind speed at the altitude 120 m depending on the fetch length for all profiles (the distance from the coast along the wind direction). No systematic behaviour is obvious. The large scatter indicates that more parameters are necessary to understand the development of wind speed with fetch length. One of them is stability.

- Line 185: What is "cut-in speed"?

We changed the text to: "The typical cut-in speed at which offshore wind turbines start producing power is around $3 \, \mathrm{m \, s^{-1}}$."

- Section 5.3: Here again, it might be more insightful to look at some statistic (e.g. ratio of wind at 50 m to wind at 100 m) as a function of other variables and/or location.

As discussed above, we would prefer to leave statistical information to dedicated studies, as the interactions require complex analyses of different parameters. We added an example of the modification of the wind speed by coastal effects:

"The profiles of temperature and wind speed are modified by coastal effects (e.g. **??**). During the WIPAFF campaign, climb and descent flights were performed on the way to the wind park measurement area and back. As an example of current and future research, the modification of the wind by coastal effects was investigated. Figure **??** shows the difference of the wind speed at hub height (120 m) for each profile minus the wind spee at hub height obtained during the profile closest to the coast. The fetch length is defined as the mean length that the air travelled above open water along the wind direction. Only flights are included where it was possible to determine the fetch length (not from North and West, as the distances to the next coast lines are too large). There is a large scatter in the data. Figure **??** shows the same data points. However, they are grouped by wind direction. There is still large scatter in the different data sets. However, depending on wind direction, the wind speed either increases or decreases with fetch length. This shows that there are more parameters required to explain the modification of wind speed besides the fetch length. A weakness of this analysis is that the profiles were not obtained along the mean wind direction. So air masses do not have the same origin, and besides the fetch length, variability along the coast line influences the results. More investigation is required to understand and parameterize the coastal effect."

- Line 189: Am I understanding correctly that these profiles include all data, and aren't necessarily at a single location? This makes these very difficult to interpret.

Yes, all available data of the vertical profiles are included, irrespective of the location. The figures intend to provide a rough overview of the meteorological conditions encountered during the campaigns. However, other ways of presentation (e.g. scatter plots) seem even more difficult to interpret, see above.

- Lines 191-192: This could be a very interesting 3-component plot (e.g. a scatter plot of wind direction vs. strength, color-coded by stability).

As described above, we included an example of the coastal effect. Fig. 3 shows the same information as Fig. 2, with additional information on the wind direction. The linear regressions are very different for each wind sector than for all data points. How-

ever, the scatter of the data points is still very large.

120   *- Lines 195-196: For unstable conditions, wouldn't you expect that mixing would result in an adiabatic profile that has an increasing RH with height?*

We agree with the referee, and changed the sentence to: "For unstable conditions, an enhanced water vapour mixing ratio directly above the water surface was present. "

125   *- Line 196: Is the increasing humidity with altitude for stable profiles the result of layered advection impacting temperature, or are there moisture plumes being advected? Or something else?*

We changed the sentence to: "For stable conditions, humidity was often increased at higher altitudes, which in most cases is most likely caused by advection of air masses with higher water vapour mixing ratio."

130   *- Section 6: I would have liked to have seen a bit more information in this conclusion. Some discussion on other complementary datasets, how these are expected to be used, etc. could be useful.*

We added in the conclusion section: "The unique data has been the base for different studies, proving for the first time directly the horizontal extension of wakes downwind of offshore wind parks (Platis et al., 2018), quantifying the recovery of wind speed in dependence of stability (Cañadillas et al., 2019; Platis et al., 2019a), and for the validation of the WRF mesoscale

135   model (Siedersleben et al., 2018a, b, 2019), which can then be used for larger scales and scenario calculations."

Also, surprisingly, there was no mention of anything going wrong/not working/etc. during the campaign, which would be very remarkable for a campaign of this extent. Did anything go wrong that the reader should know about?

We changed the text to: " Altogether, 41 measurement flights were conducted during different seasons, wind direction, wind

140   speed and stability. An overview of the flights performed during WIPAFF and meteorological conditions is shown in Tab. 1 and 2. A map with all flight paths flown during WIPAFF is provided in Fig. 3. During the flights, no instrument failures occurred. Only during one flight, the data acquisition had to be re-started (Flight 35)."

Technical Corrections:

145   *- None at this time. The grammar, while sometimes different than I would have personally used, is perfectly suitable and readable. Perhaps the editorial team finds reasons to reword/correct, but I did not come across anything that required being corrected/changed.*

Thank you!

2 Answers to referee 2

150 The authors would like to thank Christof Lüpkes for the interesting comments.

In the following, each comment is addressed. The comments are given in italic, and the answers are given in normal letters. Changes to the text are provided in quotation marks.

155 *General*
In this paper an aircraft campaign is described, which has been carried out in 2016 over North Sea in the environment of wind parks. The instrumentation, flight patterns and data sets are explained, which have been made publicly available in the world data center PANGAEA. The paper is generally well written and the unique data sets will be helpful to better understand the impact of wind turbines on atmospheric processes and the water surface. I recommend publication after some revisions
160 *mentioned below have been carried out.*
We would like to thank the referee for the positive feedback.

Revisions 1) I understand that the goal of the authors is to just describe the data sets and to leave the interpretation to later work. However, it might be possible to show in this paper at least one example illustrating the impact of the wind parks, which
165 *is missing in the current version. This would attract more readers.*
We included an example of changes of the wind when crossing the coast line. The analyses show that the development of the wind profiles from the coast to the open sea are difficult to understand and require more detailed analyses.

2) Figures 5 and 6 show an unusual structure of the atmospheric boundary layer (ABL). The authors interpreted the peak
170 *at 500 m as the ABL top. Usually, a capping inversion is found at the top but here, at least in the average profile, the contrary (unstable stratification) is found. Even more pronounced is such a behavior at 950 m. This situation needs to be explained. I recommend showing two or three examples of individual (thus non-averaged) profiles in addition, since this might help to understand the mean profiles.*
We included individual profiles of Flight 7 (stable), Flight 15 (unstable), Flight 31 (stable) in the figures of temperature, poten-
175 tial temperature, water vapour mixing ratio and wind speed.
We added in the text:
"Below 60 m, data are only available during take-off and landing. Therefore, the temperature inversion below 60 m is not a typical feature above the North Sea, and therefore provided as dotted line. The averaged and maximum temperature profiles show a sudden decrease at an altitude of around 500 m and around 950 m. This is probably an artifact from the averaging
180 method, and it is not visible in individual temperature profiles."
"In the mean profile of the potential temperature, a clear increase is observed for the altitude interval 60 to 100 m. Also up to the altitude of 200 m, in the range of the rotor blades, an overall small increase of potential temperature with height is observed.

The decrease of average and maximum potential temperatures with height at around 500 m and 950 m are probably artifacts form the averaging method and are not visible in the profiles of individual flights."

185

3) Measurements below 50 m height are obtained during take-off or landing and thus over land. So, it has nothing to do with the situation over sea and therefore, I would either mark these results with another color or skip them since this might lead to misinterpretation. The average surface temperature is however interesting, but again, the land part should be excluded from the average.

190 We now provide the profiles below 60 m, which were obtained above land during take-off and landing, in dotted lines.

4) The language is ok in general, but I found some misprints and also some unclear sentences:

line 9: it should be written ...data set has been shown already by...

We changed as suggested.

195

line 27: submitted by Baerfuss

We did as suggested.

line 29: as well as for (skip 'a')

200 Done.

line 30: WIPAFF has been...

Done.

line 37: probably, the authors mean resolution is more than 1 m (or larger than...)

205 We changed the text to "the spatial resolution of the measurements is better than 1 m"

line 39: and in particular over the sea ice...

We changed as suggested.

210 *line 58: meteorological*

We corrected the spelling.

line 60: sentence with resolution is a repetition of the introduction. The corresponding sentence of the introduction could perhaps occur here (?)

215 We moved the sentence from the earlier section here as suggested.

line 73: give value of kappa.

We changed the text to: "κ is the heat capacity ratio with a value of 1.4."

Line 105: and to derive

220 We changed the text to: "The scanning laser system VZ-1000 of Riegl, Austria, is deployed to record the relative sea surface deflection and to derive parameters like the significant wave height."

Line 112: explain sigma

We changed the text to: "since this simple calculus only depends on the standard deviation σ_η in sea surface deflection"

225

line 142: instead of behind write 'downstream'

We changed as suggested.

line 165: I do not really understand the double averaging procedure for mean values. Does the first average mean the appli-
230 *cation of a filter so that, e.g., 1 Hz data result?*

To clarify, we changed the text to: "During each flight, different vertical profiles were obtained. First, a mean profile for each flight was calculated. Then all 41 profiles from the 41 flights were averaged again. The minimum and maximum values are combined from the 41 mean profiles."

235 *line 166: Not completely clear how to understand the minimum and maximum. At each height, the minimum and maximum values were determined from all available profiles together?*

We changed the text to: "For each height, the minimum and maximum values were determined from the 41 profiles representing each one particular flight."

240 *Line 206: better write something like: data base to date, from which the impact.... can be derived.*

We changed the text to: "The WIPAFF flights are the only available data base to date, from which the impact of long-range wakes can be derived systematically and independent of infrastructural constraints like the location of masts."

Figures: Figures 3 and 4: use text size for label size as in the other figures. Times cannot be read. Either skip them or
245 *mark them in a different manner. German headings should be skipped as well and information should be given in the captions.*
Explain scale for wind speed.

We now use larger label size and omitted the times and the German headings. The colours indicating the altitude and the indications for wind direction are explained in the caption: "The colours show the flight altitude. The wind barbs indicate wind direction and a first idea of wind speed, which is proportional to the length of the wind barbs."

References

Cañadillas, B., Foreman, R., Barth, V., Siedersleben, S.K., Lampert, A., Platis, A., Djath, B., Schulz-Stellenfleth, J., Bange, J., Emeis, S., and Neumann, T.: Offshore wind farm wake recovery: Airborne measurements and its representation in engineering models, accepted to Wind Energy, 2019.

Corsmeier, U., Hankers, R., and Wieser, A.: Airborne turbulence measurements in the lower troposphere onboard the research aircraft Dornier 128-6, D-IBUF, Meteorol. Z., 10, 315-329, 2001.

Platis, A., Siedersleben, S., Bange, J., Lampert, A., Bärfuss, K., Hankers, R., Cañadillas, B., Foreman, R., Schulz-Stellenfleth, J., Djath, B., Neumann, T., and Emeis, S.: First in situ evidence of wakes in the far field behind offshore wind farms, Scientific Reports, doi 10.1038/s41598-018-20389-y, 2018.

Platis, A., Hundhausen, M., Siedersleben, S., Emeis, S., Lampert, A., Bärfuss, K., Djath, B., Schulz-Stellenfleth, J., Neumann, T., Cañadillas, B., and Bange, J.: Evaluation of a simple analytical model for offshore wind farm wake recovery by in-situ data and WRF simulations, Wind Energy, under review, 2019.

Platis, A., Siedersleben, S., Hundhausen, M., Bärfuss, K., Cañadillas, B., Schulz-Stellenfleth, J., Djath, B., Lampert, A., Neumann, T., Bange, J., and Emeis, S.: Long-range modifications of the wind field by offshore wind parks - results of the project WIPAFF, submitted to Meteorologische Zeitschrift, 2019.

Siedersleben, S.K., Platis, A., Lundquist, J.K., Lampert, A., Bärfuss, K., Cañadillas, B., Djath, B., Schulz-Stellenfleth, J., Neumann, T., Bange, J., and Emeis, S.: Evaluation of a Wind Farm Parametrization for Mesoscale Atmospheric Flow Models with Aircraft Measurements, Meteorologische Zeitschrift, PrePub DOI 10.1127/metz/2018/0900, 2018a.

Siedersleben, S.K., Lundquist, J.K., Platis, A., Bange, J., Bärfuss, K., Lampert, A., Cañadillas, B., Neumann, T., and Emeis, B.: Micrometeorological impacts of offshore wind farm as seen in observations and simulations, Env. Res. Lett., 13, 124012, 2018b.

Siedersleben, S.K., Platis, A., Lundquist, J.K., Djath, B., Lampert, A., Bärfuss, K., Cañadillas, B., Schultz-Stellenfleth, J., Bange, J., Neumann, T., and Emeis, B.: Observed and simulated turbulent kinetic energy (WRF 3.8.1) overlarge offshore wind farms, Geosci. Model Dev. Discuss., https://doi.org/10.5194/gmd-2019-100, in review, 2019.
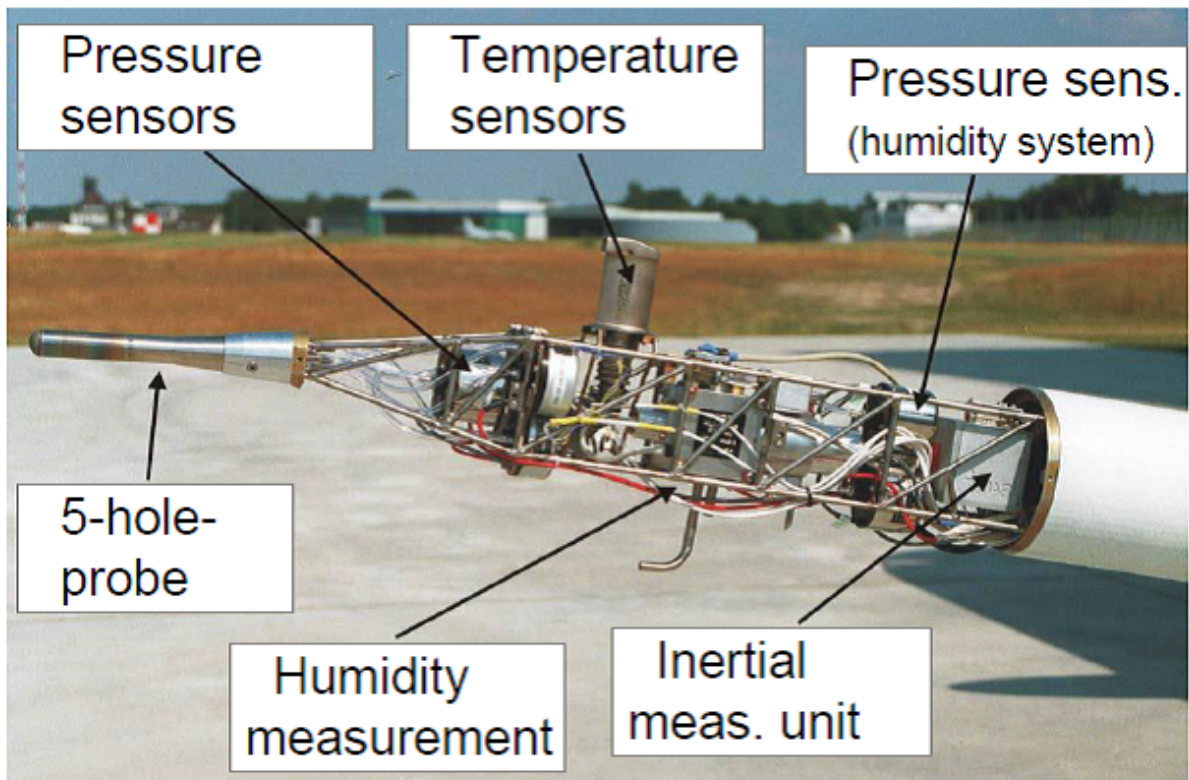
Figure 1. Nose boom and instrumentation of the research aircraft Dornier 128-6 D-IBUF. Photo: Mark Bitter, TU Braunschweig
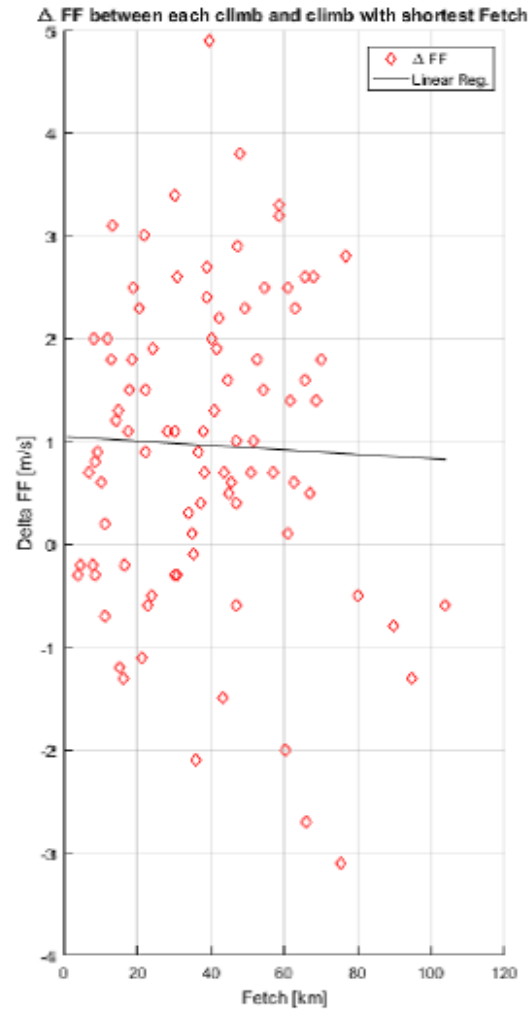
Figure 2. Change of the wind speed depending on the fetch length (distance to coast along wind direction) for the altitude 120 m.
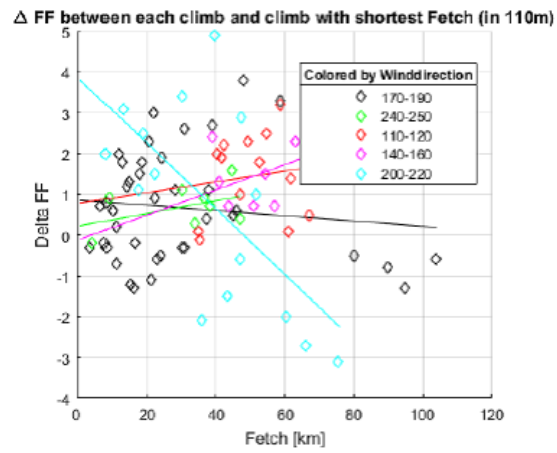
Figure 3. Change of the wind speed depending on the fetch length (distance to coast along wind direction) for the altitude 120 m (same as Fig. 2). The colours indicate the sector of the wind direction.

In-situ airborne measurements of atmospheric and sea surface parameters related to offshore wind parks in the German Bight

Astrid Lampert[1], Konrad Bärfuss[1], Andreas Platis[2], Simon Siedersleben[3], Bughsin Djath[4],
Beatriz Cañadillas[5], Robert Hunger[1], Rudolf Hankers[1], Mark Bitter[1], Thomas Feuerle[1], Helmut Schulz[1],
Thomas Rausch[1], Maik Angermann[1], Alexander Schwithal[1], Jens Bange[2],
Johannes Schulz-Stellenfleth[4], Thomas Neumann[5], and Stefan Emeis[3]

[1]Institute of Flight Guidance, Technische Universität Braunschweig, Braunschweig, Germany
[2]Eberhard Karls University, Tübingen, Germany
[3]Karlsruhe Institute of Technology, Garmisch-Partenkirchen, Germany
[4]Helmholtz-Zentrum Geesthacht, Institute of Coastal Research, Geesthacht, Germany
[5]UL International, Oldenburg, Germany

Correspondence: Astrid Lampert (Astrid.Lampert@tu-braunschweig.de)

Abstract. Between 6 September 2016 and 15 October 2017, meteorological measurement flights were conducted above the German Bight in the framework of the project WIPAFF (Wind Park Far Field). The scope of the measurements was to ~~investigate~~ study long-range wakes with extent larger than 10 km behind entire wind parks, and to investigate the interaction of wind parks and the marine atmospheric boundary layer. The research aircraft Dornier 128 of TU Braunschweig

5 performed in total 41 measurement flights during different seasons and different stability conditions. The instrumentation consisted of a nose boom with sensors for measuring the wind vector, temperature and humidity, and additionally sensors for characterizing the water surface, a surface temperature sensor, a laser scanner, and two cameras in the visible and infrared wavelength range. A detailed overview of the aircraft, sensors, data post processing and flight patterns is provided here. Further, averaged profiles of atmospheric parameters illustrate the range of conditions. The potential use of the data set

10 ~~is shown~~ has been shown already by first publications. The data are publicly available in the world data center PANGAEA (https://doi.org/10.1594/PANGAEA.902845, Bärfuss et al., 2019a).

1 Introduction

The growing demand in renewable energy has led to large-scale installations of wind parks in the German Bight in the last decades. Before the project WIPAFF, satellite images of synthetic aperture radar (SAR) indicated modifications of the sea

15 surface up to several 10 km downstream of wind parks (Christiansen and Hasager, 2005; Li and Lehner, 2013). Also numerical simulations suggested the existence of far-reaching wake areas with reduced wind speed and enhanced turbulence (Fitch et al., 2012). Motivated by these results~~and the missing~~, the lack of in-situ evidence and the need of understanding the wake effects as well as to collect in-situ data to validate existing wakes models, the project WIPAFF (Wind Park Far Field) was funded by the German Federal Ministry for Economic Affairs and Energy (BMWi). To verify these indirect es-

20 timates and quantify the effects of wind parks on the marine atmospheric boundary layer, flight measurements were per-

1

formed. Within the project WIPAFF, the flights were embedded in further stationary measurements of wind profiles by wind lidar systems and meteorological tower measurements at the masts FINO1 and FINO3. Satellite images provided statistical information on wake occurrence and extensions. WRF simulations were performed for ~~the~~ some measurement flights, and verified by the observations. First results of the measurements have been presented in Platis et al. (2018), and WRF simulations and validation with observational data have been presented in Siedersleben et al. (2018a, b, 2019). The importance of atmospheric stability for the development of wakes has been addressed by Platis et al. (2019b) and will be investigated in detail in another publication. Analyses of wake recovery ~~have~~ as a function of atmospheric stability and its representation in engineering model has been addressed by Cañadillas et al. (2020). The validation of an analytical model has been submitted by ~~Cañadillas et al. (2020); Platis et al. (2019a)~~ Platis et al. (2019a). An intercomparison of the significant wave height obtained by the airborne laser scanner and a wave model has been submitted ~~Bärfuss et al. (2019b)~~ by Bärfuss et al. (2019b). Analyses of large-scale wakes as a function of atmospheric stability by satellite remote sensing are published in Djath et al. (2018). For describing the surface roughness, airborne laser scanner data have been used to fill the gap between buoy and satellite observations, as well as ~~a~~ for validation of wave simulations in the German Bight (Bärfuss et al., 2019b). An overview publication of the main results of the project WIPAFF ~~have~~ has been submitted (Platis et al., 2019b).

2 Research aircraft Dornier-128

The airborne measurements were performed with the research aircraft Dornier 128-6 with call sign D-IBUF. The Dornier 128-6 is a twin-engined turboprop powered research aircraft used for different research fields (Fig. 1). Besides all necessary avionic instrumentation for flights especially at very low altitudes it has versatile sensor equipment combined with a powerful data acquisition system. ~~With a mean ground speed of about 65 m s^{-1} and a measuring rate of 100 Hz the spatial resolution of the measurements is less than 1 m.~~ The Dornier 128-6 has been used for different kind of meteorological research, in particular for investigations of processes in the atmospheric boundary layer (ABL):

Several measurement campaigns were performed above the North Polar Ocean, the Golf of Bothnia and in particular over the sea ice edge with the aim to investigate meteorological processes at the intersection of sea ice and open water for off-ice flow, resulting in convective cells and cloud streets (Brümmer et al., 1994, 2002). The aircraft was used for studying the sources and chemical cycle of anthropogenic ozone in the ABL (Corsmeier et al., 2002). The impact of inhomogeneous terrain on the turbulent exchange processes between ground and the atmospheric boundary layer was investigated by Bange et al. (2002, 2006). Convective processes up to the formation of thunderstorms in the atmosphere were studied by direct measurements in the clouds and drop sondes released from the aircraft (Groenemeijer et al., 2009). The aircraft was deployed above the Mediterranean to investigate cyclones and mesoscale convective systems to understand which atmospheric conditions lead to devastating thunderstorms, and to improve the forecasting of such systems (Drobinski et al., 2013; Ducrocq et al., 2013; Sodemann et al., 2017). A comparison of convective boundary layer conditions between wind lidar and airborne measurements was performed (Adler et al., 2019). The aircraft was used for an intercomparison of fast humidity sensors (Lampert et al., 2018). There is an online graphical display with time series and vertical profiles of all important measured and calculated meteorolog-

ical parameters (wind speed, wind direction, turbulent kinetic energy, eddy dissipation rate, temperature, potential temperature, humidity, surface temperature), enabling the onboard scientist to modify the ongoing mission based on the measured parameters, if necessary. Like this, it was possible to adapt the flight pattern during the mission. For the flights at the wind parks at low altitudes down to 60 m, a special permission was required.

In the data set, the aircraft position, altitude, velocity in all three directions, the pitch and roll angle and heading are provided, which are necessary for the data analyses. Further, the radar altitude above ground is given.

3 Sensors and data processing

For ~~meteorologicaal~~ meteorological flight campaigns, the Dornier-128 aircraft can be equipped with a nose boom and additional sensors. The sensor system is specialized for meteorological measurements (Corsmeier et al., 2001); the central sensor package is contained in the nose boom (Fig. 2). This concentration of meteorological sensors with high temporal resolution for measuring temperature, humidity, wind speed and wind direction leads to a high spatial resolution of the data. With a mean ground speed of about $65 \, \text{m s}^{-1}$ and a measuring rate of 100 Hz the spatial resolution of the measurements is higher than 1 m. The application of the nose boom for measuring the wind vector, temperature and humidity, and the surface temperature sensor represent standard research components of the Dornier-128. The laser scanner for sea surface deflection and nadir looking cameras were integrated specifically for the WIPAFF campaigns. In the following, the sensors and the standard calibration procedures are presented.

3.1 Temperature

Temperature measurements are performed by two complementary sensors, the slow, but highly accurate 102DB1AG temperature sensor (Rosemount, US) with an accuracy of ± 0.1 K, and the 102E4AL sensor (Rosemount, US) with a fast response time and an accuracy of ± 0.25 K plus 0.5% of the temperature to be measured in $^\circ$C. The slow sensor is heatable, but heating was not switched on, as no icing conditions were present during the flights.

The total temperature T_{total} is derived by applying a recovery factor to the raw measurements to compensate the self heating effect. From the total temperature in K, the static temperature T_{stat} in K is derived adiabatically (Stickney et al., 1994):

$$T_{stat} = T_{total} \cdot \left(\frac{p_{stat}}{p_{total}} \right)^{\frac{\kappa - 1}{\kappa}} \tag{1}$$

Here, p_{stat} is the static pressure and p_{total} is the total pressure, the sum of static and dynamic pressure. κ is the ~~hear capacity ratio~~ heat capacity ratio with a value of 1.4.

The calibration of the temperature sensors is done by applying specific resistance values corresponding to specific temperatures as stated by the manufacturer.

In the PANGAEA data set Bärfuss et al. (2019a), the static air temperature derived from the fast sensor is provided, after using the slow sensor for quality check. The parameter is simply called "air temperature".

3.2 Humidity

For measuring humidity, three different measurement principles are used: A capacitive Vaisala Humicap HMP233, Finland, a dew point mirror TP 3-S of Meteolabor, Switzerland, and a Lyman-Alpha optical sensor L-6 / HMS-2 of Buck Research, US. The humidity sensors have a joint heatable inlet, and other parameters like temperature and pressure are recorded for the humidity channel as well. The humidity sensors are cleaned and calibrated before each meteorological measurement campaign by applying saturated salt solutions with known relative humidity in an equilibrium state. In the PANGAEA data set, the relative humidity of the dew point mirror is provided as a reference with good accuracy of the absolute values (accuracy of the dew point specified by the manufacturer as 0.15 K) The temporal resolution is composed of a time <0.5 s for the condensation process or temperatures above $0°$ C, plus a time delay proportional to the magnitude of abrupt changes in the dew point (5 K s^{-1}). The relative humidity of the Lyman-Alpha sensor with much shorter response time is provided for deriving fluctuations.

3.3 Pressure and wind

With the 5-hole probe of Rosemount, US, and pressure transducers of Setra, US, the static and dynamic pressure, as well as the air flow angles are retrieved in the aircraft-fixed coordinate system. All inertial data (position, ground speed, Eulerian angles) were derived from the complementary use of the inertial measurement platform iNAV-RQH-1003 of iMAR, Germany, operated in parallel to the former standard system Lasernav of Honeywell, US, and a NovAtel GPS OEM-6, Canada. These input parameters are then used to calculate the wind vector according to the formulation in Lenschow (1972), whereas the fundamental vector difference equation in geodetic coordinates is

$$\overline{V}_{w_g} = \overline{V}_{K_g} - \overline{V}_g \tag{2}$$

$\overline{V}_{w_g}$ denotes the wind vector, $\overline{V}_{K_g}$ the flight path velocity, and $\overline{V}_g$ the velocity vector of the aircraft with respect to the air. In the PANGAEA data set, all three components of the wind vector are provided at 100 Hz resolution to derive horizontal wind speed, wind direction and turbulent properties. Further, the air density derived from the static pressure and temperature is given.

3.4 Sea surface temperature

An infrared KT15.82D sensor of Heimann, now Heitronics, Germany, is used to determine the surface temperature. It has an accuracy of ± 1.2 K at $20°$ C surface temperature and a temporal resolution of 20 Hz. If no clouds are between the sensor and the surface, the surface temperature measurements are not influenced by the atmospheric temperature or humidity distribution. The footprint size is 10 m at a distance of 900 m for the specific system. In the PANGAEA data set, the parameter is called surface temperature.

3.5 Sea surface deflection

The scanning laser system VZ-1000 of Riegl, Austria, is deployed ~~for recording~~ to record the relative sea surface deflection and to derive parameters like the significant wave height. ~~From the distance measurements along beam direction~~

From the point measurements in the scanner's coordinate system $\begin{pmatrix} v_{x_{body}} \\ v_{y_{body}} \\ v_{z_{body}} \end{pmatrix}$, aircraft attitude corrections using Eulerian angles Ψ, Θ, Φ are applied to rotate aircraft body fixed coordinates into the geodetic coordinate system (positive directions East, North, Up), which then are geolocated by applying the aircraft position $\begin{pmatrix} p_{x_{body}} \\ p_{y_{body}} \\ p_{z_{body}} \end{pmatrix}$ in the following manner:

$$\begin{pmatrix} p_{x_{geo}} \\ p_{y_{geo}} \\ p_{z_{geo}} \end{pmatrix} = R_{geo}^{body}(-\Psi, -\Theta, -\Phi) \begin{pmatrix} v_{x_{body}} \\ v_{y_{body}} \\ v_{z_{body}} \end{pmatrix} \pm \begin{pmatrix} p_{x_{body}} \\ p_{y_{body}} \\ p_{z_{body}} \end{pmatrix} \tag{3}$$

Subsequently, the surface deflection η is calculated ~~using aircraft attitude corrections~~out of the georeferenced point cloud using mean sea level. The system's effective rate of the distance measurements is up to $122\,\mathrm{kHz}$, but decreases over water because of specular reflections. Accuracy and resolution along the beam direction are stated to be less than $10\,\mathrm{mm}$, and measurements can be taken up to a distance of $450\,\mathrm{m}$ with the settings used during flight campaigns.

Significant wave height (SWH) H_s, defined in the spatial domain, is used to describe the sea surface. The approximation $H_s \approx H_{m_0} = 4 \cdot \sigma_\eta$ mentioned in Young (1999) was used, since this simple calculus only depends on the standard deviation σ_η in sea surface deflection. Here, H_{m_0} is four times the standard deviation of the sea surface deflection measurements~~σ_η~~, normally defined in the frequency domain. In this case, it is derived from measurements in the space domain. With a deflection measurement rate of more than $3\,\mathrm{kHz}$ over water, this produces stable results in SWH estimation. As scan pattern, a line scan pattern rectangular to the flight direction was used, which provides a spatial resolution of about $0.5\,\mathrm{m}$ x $0.5\,\mathrm{m}$ between measurement points perpendicular to and along the flight trajectory. In the PANGAEA data set sea surface deflections η are analysed for standard deviation within a time window of $10\,\mathrm{s}$.

3.6 Cameras

Two downward looking cameras, one for the visible wavelength range (MV1-D1312-G2 of Photonfocus, Switzerland), and one for the infrared range (A35SC of FLIR, Germany) were deployed in the fuselage to document the sea surface. The images are influenced by sun glint and by varying cloud cover. The exposure time of the visible camera was adapted manually. The retrieval of specific parameters requires additional intensive processing of the images.

The large data sets are available at the Institute of Flight Guidance upon request. They are not included in the data base. Further,

handheld cameras were used to document the overall impression, clouds and special features. They are not included in the data base either.

4 Flight planning and flight patterns

140 In preparation of the measurement campaign, flight patterns were programmed to systematically probe the far field wakes behind the wind ~~parks~~ park clusters including Godewind and Amrumbank West (named N-3 and N-4 according the offshore areas specified by the German Federal Hydrographic Agency) for different wind directions every 10°. Altogether, 41 measurement flights were conducted during different seasons, wind direction, wind speed and stability. An overview of the flights performed during WIPAFF and meteorological conditions is shown in Tab. 1. A map with all flight paths flown during WIPAFF is pro-

145 vided in Fig. 3. ~~Flights~~ During the flights, no instrument failures occurred. Only during one flight, the data acquisition had to be re-started (Flight 35).

Generally, flights were performed downwind of Amrumbank West for a wind direction sector of 80° to 200°, and downwind of Godewind for a sector from 160° to 350°. However, there are exceptions for particular reasons (e.g. during Flight 5 for consecutively probing the wakes of both wind parks, Flight 6 for investigating the changes of the wind field above the wind

150 park). Depending on the wind direction, either the cluster of Amrumbank West or Godewind was investigated, as flights were only performed above water and only above German controlled air space. The flight patterns were prepared with a software developed at the Institute of Flight Guidance. A special function is implemented for programming meander patterns automatically after defining a starting point and the length and distance of legs. The flights were performed from the airports Wilhelmshaven (ICAO code EDWI), Husum (EDXJ) or Borkum (EDWR) depending on wind direction and runway orientation, and proximity

155 to the wind parks. ~~An overview of the flights performed during WIPAFF and meteorological conditions is shown in Tab. 1.~~

4.1 Meander at hub height (MEANDER)

To quantify the wakes behind offshore wind parks and determine the wake length, meander flight patterns at hub height perpendicular to the prevailing wind direction were applied (MEANDER). An example is provided in Fig. 4. For these flight patterns, isolated wind parks with long distance of unobstructed water surface downwind were selected. The flight pattern typically

160 started with a leg 500 m ~~behind~~ downstream of the last wind turbines. The distance to the next flight legs was set as 10 km. The flight altitude was adapted to the hub height and was either 90 m (Amrumbank West) or 120 m (Godewind). On the way to the wind park and after the meander pattern, vertical soundings from 60 to 550 m, sometimes up to 1000 m were performed to investigate atmospheric stability. For unstable conditions, the distance between the flight legs perpendicular to the wind direction was shortened. This flight pattern was used for 26 out of the 41 flights.

165 Results of meander flight patterns have been published in Platis et al. (2018); Siedersleben et al. (2018a); Cañadillas et al. (2020).

6

4.2 ~~Cross~~ Vertical cross sections ~~through height~~ (CROSS)

To quantify the vertical extent of wakes, several cross sections at the same distance downwind of the windpark were flown perpendicular to the wake at different altitudes (CROSS). Typical flight altitudes were 60 m, 90 m, 130 m, 150 m and 200 m. On the way to the wind park and back, vertical soundings from 60 to 550 m, sometimes up to 1000 m were performed to investigate atmospheric stability. Such flight patterns were applied during 8 out of the 41 measurement flights.

Results of the cross section patterns measured on 10 September 2016 have been published in Siedersleben et al. (2018a, b).

4.3 Above wind parks (ABOVE)

To quantify the interaction of the wind parks and the atmospheric boundary layer, a flight pattern with legs upwind, above and downwind the wind park was repeated several times (ABOVE, Fig. 5). Individual flight legs had a length of 45 km. The flight pattern was flown at an altitude of 65 m above the top of the rotor blades. On the way to and from the wind park, vertical soundings were performed to obtain information on atmospheric stability.

Such flight patterns were performed during 18 out of the 41 measurement flights.

Results of the flight patterns above wind parks have been published by Siedersleben et al. (2019).

5 Atmospheric conditions

The low-level flights were conducted under visual flight conditions. A minimum visibility of 10 km, a minimum cloud ceiling of 1.000 ft and no precipitation were required. Therefore the results are not statistically representative of atmospheric conditions above the North Sea. On the contrary, in particular in spring 2017, flights were only possible on occasional days.

During the flights, a large variety of atmospheric conditions was encountered. The focus of the flight was on far reaching wakes, therefore days with very stable atmospheric conditions were the preferred option. However, for ~~comparision~~comparison, days with less stable conditions were probed as well. In the following, vertical profiles of the mean and extreme values of temperature, potential temperature, wind speed and water vapour mixing ratio are presented. ~~The mean values were obtained by averaging first over all vertical profiles during each flight , and then averaging over the resulting~~ During each flight, different vertical profiles were obtained. First, a mean profile for each flight was calculated. Then all 41 profiles ~~. The~~ from the 41 flights were averaged again. For each height, the minimum and maximum values ~~are combined~~ were determined from the 41 ~~mean profiles~~ profiles representing each one particular flight.

5.1 Temperature

The temperatures encountered during the WIPAFF flights span a broad range, as the flights were performed during different seasons. The near-surface air temperature varied between 7° C and 25° C (see Fig. 6). Overall, the temperature decreased with altitude. Below 60 m, data are only available during take-off and landing. Therefore, the temperature inversion below ~~50~~60 m is ~~probably an artifact and~~ not a typical feature above the North Sea, and therefore provided as dotted line. The averaged and

7

maximum temperature profiles show a sudden decrease at an altitude of around 500 m and around 950 m. This is probably an artifact from the averaging method, and it is not visible in individual temperature profiles.

5.2 Stability

Atmospheric stability is strongly related to season and wind direction. In spring and summer, the water surface warms relatively slowly, whereas atmospheric temperatures above land are subject to a strong diurnal cycle. Therefore, flow from land to sea during day very frequently results in stable conditions. For northerly wind directions, the air temperature is typically similar to the water surface temperature, so unstable or neutral conditions prevail. A rough overview of all conditions is indicated in Fig. 7. In the mean profile of the potential temperature, a clear increase is observed for the altitude interval ~~50~~ 60 to 100 m. Also up to the altitude of 200 m, in the range of the rotor blades, an overall small increase of potential temperature with height is observed. The decrease of average and maximum potential temperatures with height at around 500 m and 950 m are probably artifacts form the averaging method and are not visible in the profiles of individual flights.

As stability typically changes with distance to the coast and with the diurnal cycle, the categorization of the flights according to one specific stability parameter is difficult and needs thorough discussion, which is addressed in Platis et al. (2019b) and will be subject to another publication. The exact altitude of the temperature inversion in relation to the rotor geometry plays a crucial role for the modification of temperature and humidity profiles in the wake areas (Siedersleben et al., 2018b).

5.3 Wind speed

During the flights, wind speed at hub height varied between $2\,\mathrm{m\,s^{-1}}$ and $17\,\mathrm{m\,s^{-1}}$. The typical cut-in speed ~~of~~ at which offshore wind turbines start producing power is around $3\,\mathrm{m\,s^{-1}}$. The rated speed for offshore wind turbines is typically designed as $12\,\mathrm{m\,s^{-1}}$, and the cut-out speed, where wind turbines are shut down is at $25\,\mathrm{m\,s^{-1}}$. The wind speed typically increases more strongly with altitude for stable conditions. An overview of all wind speed profiles encountered during the flights is shown in Fig. 8. The strong increase of wind speed from the surface to 50 m is an artifact as these altitudes were only sampled during take-off and landing.

5.4 Wind direction

Measurement flights were performed for mean wind directions at hub height between 80° and 330°. Wind directions from NW were always associated with unstable or neutral atmospheric stability. This wind sector was investigated mainly for comparison. The main focus was on stable conditions, and therefore wind from land.

5.5 Humidity

The profiles of humidity varied strongly depending on stability. For unstable conditions, ~~a high relative humidity~~ an enhanced water vapour mixing ratio directly above the water surface was present. For stable conditions, humidity was often increased at higher altitudes, which in most cases is most likely caused by advection of air masses with higher water vapour mixing

ratio. Depending on the altitude of the temperature inversion in relation to the altitude of the rotor blades, humidity was either increased or decreased in the wake (Siedersleben et al., 2018b). As the relative humidity is temperature dependent, profiles of the water vapour mixing ratio are shown in Fig. 9. The water vapour mixing ratio varied between 2 and $14\,\mathrm{g\,kg^{-1}}$. For the mean profile, a sharp decrease of the mixing ratio with altitude is present at around $500\,\mathrm{m}$. This corresponds to the altitude with a change of stability as indicated by the potential temperature and an increase in the wind speed, indicating the mean altitude of the marine atmospheric boundary layer.

For completeness and for interpretation of the data, the prevailing cloud conditions based on visual observations are indicated in Table 1 and 2.

6 Modification of wind field by the coast

The profiles of temperature and wind speed are modified by coastal effects (e.g. Dörenkämper et al. (2015); van der Laan et al. (2017)). During the WIPAFF campaign, climb and descent flights were performed on the way to the wind park measurement area and back. As an example of current and future research, the modification of the wind by coastal effects was investigated. Figure 10 shows the difference of the wind speed at hub height ($120\,\mathrm{m}$) for each profile minus the wind spee at hub height obtained during the profile closest to the coast. The fetch length is defined as the mean length that the air travelled above open water along the wind direction. Only flights are included where it was possible to determine the fetch length (not from North and West, as the distances to the next coast lines are too large). There is a large scatter in the data. Figure 11 shows the same data points. However, they are grouped by wind direction. There is still large scatter in the different data sets. However, depending on wind direction, the wind speed either increases or decreases with fetch length. This shows that there are more parameters required to explain the modification of wind speed besides the fetch length. A weakness of this analysis is that the profiles were not obtained along the mean wind direction. So air masses do not have the same origin, and besides the fetch length, variability along the coast line influences the results. More investigation is required to understand and parameterize the coastal effect.

7 Conclusions

The WIPAFF flights are the only available data ~~base to datethat directly measure~~ set to date, from which the impact of long-range wakes can be derived systematically and independent of infrastructural constraints like the location of masts. Under stationary conditions, the aircraft data provide detailed information on the modifications of the flow field downstream of wind parks. For the interpretation, spatial changes in the flow field caused by synoptic-scale differences have to be taken into account, e.g. North-South gradients in wind speed and wind direction. ~~Further, the wind field is influenced by coastal effects.~~ Also temporal changes of the wind field have to be taken into account for the four-hour flights. During this time period, stationary conditions cannot always be assumed. For the data interpretation, short-time changes as frontal systems, synoptic-scale continuous changes, and modification of air masses and stability due to the diurnal cycle of solar radiation have to be considered. The data set can be used complementary to other wind field observations by satellite, at the wind parks and for lidar measure-

ments and to validate specific results, as suggested by Schneemann et al. (2019).

The unique data has been the base for different studies, proving for the first time directly the horizontal extension of wakes
260 downwind of offshore wind parks (Platis et al., 2018), quantifying the wind speed recovery in dependence of stability (Cañadillas et al., 202
and for the validation of the WRF mesoscale model (Siedersleben et al., 2018a, b, 2019), which can then be used for larger
scales and future wind energy scenario calculations.

8 Data availability

The data are publicly available at https://doi.pangaea.de/10.1594/PANGAEA.902845 (Bärfuss et al., 2019a). Each data set of
265 a flight in ascii format as tab-delimited text has a size of around 140 MB. The zip file containing all data sets as tab-delimited
text has a size of around 750 MB. Upon request, additional laser scanner raw data, camera images in the visible and infrared
wavelength range and manual cloud photographs are available. Satellite images of Sentinel-1 (A and B) and are freely available
at https://scihub.copernicus.eu/.

References

Adler, B., Kisileva, O., Kalthoff, N., and Wieser, A.: Comparison of Convective Boundary-layer Characteristics from Aircraft and Wind Lidar Observations, J. Tech., https://doi.org/10.1175/JTECH-D-18-0118.1, 2019.

Bange, J., Beyrich, F., and Engelbart, D.A.M.: Airborne measurements of turbulent fluxes during LITFASS-98: Comparison with ground measurements and remote sensing in a case study, Theor. Appl. Climatol., 73, 35-51, 2002.

Bange, J., Zittel, P., Spiess, T., Uhlenbrock, J., and Beyrich, F.: A new method for the determi-nation of area-averaged turbulent surface fluxes from low-level flights using inverse models, Bound.-Layer Meteorol., 119, 527-561, 2006.

Bärfuss, K., Hankers, R., Bitter, M., Feuerle, T., Schulz, H., Rausch, T., Platis, A., Bange, J., and Lampert, A.: In-situ air-borne measurements of atmospheric and sea surface parameters related to offshore wind parks in the German Bight, PANGAEA, https://doi.pangaea.de/10.1594/PANGAEA.902845, 2019.

Bärfuss, K.B., Djath, B., Lampert, A., and Schulz-Stellenfleth, J.: Airborne LiDAR Measurements of the sea surface properties in the German Bight, submitted to Transactions on Geoscience and Remote Sensing, 2019.

Brümmer, B., Busack, B., and Hoeber, H: Boundary-Layer Observations over water and Arctic sea ice during on-ice air flow, Boundary-Layer Meteorol., 68, 75-108, 1994.

Brümmer, B., Kirchgäßner, A., Müller, G., Schröder, D., Launiainen, J., and Vihma, T.: The BALTIMOS (BALTEX Integrated Model System) field experiments: A comprehensive atmospheric boundary layer data set for model validation over the open and ice-covered Baltic Sea, Boreal Environ. Res., 7, 371-378, 2002.

Cañadillas, B., Foreman, R., Barth, V., Siedersleben, S.K., Lampert, A., Platis, A., Djath, B., Schulz-Stellenfleth, J., Bange, J., Emeis, S., and Neumann, T.: Offshore wind farm wake recovery: Airborne measurements and its representation in engineering models, Wind Energy, ~~under review, 2019.~~ DOI: 10.1002/we.2484, 17 pp., 2020.

Christiansen, M.B., and Hasager, C.B.: Wake effects of large offshore wind farms identified from satellite SAR, Remote Sens. Environ., 98, 251-268, doi:10.1016/j.rse.2005.07.009, 2005.

Corsmeier, U., Hankers, R., and Wieser, A.: Airborne turbulence measurements in the lower troposphere onboard the research aircraft Dornier 128-6, D-IBUF, Meteorol. Z., 10, 315-329, 2001.

Corsmeier, U., Kalthoff, N., Vogel, B., Hammer, M.-U., Fiedler, F., Kottmeier, C., Volz-Thomas, A., Konrad, S., Glaser, K., Neininger, B., Lehning, M., Jaeschke, W., Memmesheimer, M., Rapenglück, B., and Jakobi, G.: Ozone and PAN Formation Inside and Outside of the Berlin Plume – Process Analysis and Numerical Process Simulation, J. Atmos. Chem., 42, 289-321, 2002.

Djath B., Schulz-Stellenfleth, J., and Canadillas, B.: Impact of atmospheric stability on X-band and C-band Synthetic Aperture Radar imagery of offshore windpark wakes, Journal of Sustainable and Renewable Energy, 10, 043301, doi: 10.1063/1.5020437, 2018.

Dörenkämper, M., Optis, M., Monahan, A., and Steinfeld, G.: On the Offshore Advection of Boundary-Layer Structures and the Influence on Offshore Wind Conditions, Boundary-Layer Meteorol 155, 459–482, https://doi.org/10.1007/s10546-015-0008-x, 2015.

Drobinski, P. Ducrocq, V., Albert, P., et al.: HyMeX, a 10 year multidisciplinary program on the Mediterranean water cycle, Bull. Amer. Meteor. Soc., early online view, DOI: 10.1175/BAMS-D-12-00242.1, 2013.

Ducrocq, V., Braud, I., Davolio, S., et al.: HyMeX-SOP1, the field campaign dedicated to heavy precipitation and flash flooding in the northwestern Mediterranean, Bull. Amer. Meteor. Soc., early online view, DOI: 10.1175/ BAMS-D-12-00244.1, 2013.

Emeis, S., Siedersleben, S., Lampert, A., Platis, A., Bange, J., Djath, B., Schulz-Stellenfleth, J., and Neumann, T.: Exploring the wakes of large offshore wind farms, Journal of Physics: Conference Series, IOP Publishing, 753, 092014, doi:10.1088/1742-6596/753/9/092014, 2016.

315 Fitch, A.C., Olson, J.B., Lundquist, J.K., Dudhia, J., Gupta, A.K., Michalakes, J., and Barstad, I.: Local and Mesoscale Impacts of Wind Farms as Parameterized in a Mesoscale NWP Model. Mon. Wea. Rev., 140 (9), 3017–3038, doi:10.1175/MWR-D-11-00352.1, 2012.

Foreman, R., Cañadillas, B., Neumann, T., and Emeis, S.: Measurements of heat and humidity fluxes in the wake of offshore wind turbines, J. of Renewable and Sustainable Energy, 9, 053304, 2017.

Groenemeijer, P., Barthlott, C., Behrendt, A., Corsmeier, U., Handwerker, J., Kohler, M., Kottmeier, C., Mahlke, H., Pal, S., Radlach, M.,
320 Trentmann, J., Wieser, A., and Wulfmeyer, V.: Observations of Kinematics and Thermodynamic Structure Surrounding a Convective Storm Cluster over a Low Mountain Range, Monthly Weather Review, 137, 585-602, 2009.

van der Laan, M.P., Peña, A., Volker, P., Hansen, K.S., Sørensen, N.N., Ott, S., and Hasager, C.B.: Challenges in simulating coastal effects on an offshore wind farm, IOP Conf. Series: Journal of Physics: Conf. Series, 854, 012046, doi:10.1088/1742-6596/854/1/012046, 2017.

Lampert, A., Hartmann, J., Pätzold, F., Lobitz, L., Hecker, P., Kohnert, K., Larmanou, E., Serafimovich, A., and Sachs, T.: Comparison of
325 Lyman-alpha and LI-COR infrared hygrometers for airborne measurement of turbulent fluctuations of water vapour, Atmos. Meas. Tech., 11, 2523–2536, 2018.

Lenschow, D.H.: The Measurement of Air Velocity and Temperature Using the NCAR Buffalo Aircraft Measuring System; National Center for Atmospheric Research, Boulder Colorado, NCAR-TN/EDD-74, 39, DOI:10.5065/D6C8277W, 1972

Li, X.-M., and Lehner, S.: Observation of TerraSAR-X for studies on offshore wind turbine wake in near and far fields, IEEE Journal of
330 Selected Topics in Applied Earth Observations and Remote Sensing, 6, 1757-1769, 2013.

Platis, A., Siedersleben, S., Bange, J., Lampert, A., Bärfuss, K., Hankers, R., Cañadillas, B., Foreman, R., Schulz-Stellenfleth, J., Djath, B., Neumann, T., and Emeis, S.: First in situ evidence of wakes in the far field behind offshore wind farms, Scientific Reports, doi 10.1038/s41598-018-20389-y, 2018.

Platis, A., Hundhausen, M., Siedersleben, S., Emeis, S., Lampert, A., Bärfuss, K., Djath, B., Schulz-Stellenfleth, J., Neumann, T., Cañadillas,
335 B., and Bange, J.: Evaluation of a simple analytical model for offshore wind farm wake recovery by in-situ data and WRF simulations, Wind Energy, under review, 2019.

Platis, A., Siedersleben, S., Hundhausen, M., Bärfuss, K., Cañadillas, B., Schulz-Stellenfleth, J., Djath, B., Lampert, A., Neumann, T., Bange, J., and Emeis, S.: Long-range modifications of the wind field by offshore wind parks - results of the project WIPAFF, submitted to Meteorologische Zeitschrift, 2019.

340 Schneemann, J., Rott, A., Dörenkämper, M., Steinfeld, G., and Kühn, M.: Cluster wakes impact on a far distant offshore wind farm's power, Wind Energ. Sci. Discuss., https://doi.org/10.5194/wes-2019-39, in review, 2019.

Siedersleben, S.K., Platis, A., Lundquist, J.K., Lampert, A., Bärfuss, K., Cañadillas, B., Djath, B., Schulz-Stellenfleth, J., Neumann, T., Bange, J., and Emeis, S.: Evaluation of a Wind Farm Parametrization for Mesoscale Atmospheric Flow Models with Aircraft Measurements, Meteorologische Zeitschrift, PrePub DOI 10.1127/metz/2018/0900, 2018a.

345 Siedersleben, S.K., Lundquist, J.K., Platis, A., Bange, J., Bärfuss, K., Lampert, A., Cañadillas, B., Neumann, T., and Emeis, B.: Micrometeorological impacts of offshore wind farm as seen in observations and simulations, Env. Res. Lett., 13, 124012, 2018b.

Siedersleben, S.K., Platis, A., Lundquist, J.K., Djath, B., Lampert, A., Bärfuss, K., Cañadillas, B., Schultz-Stellenfleth, J., Bange, J., Neumann, T., and Emeis, B.: Observed and simulated turbulent kinetic energy (WRF 3.8.1) overlarge offshore wind farms, Geosci. Model Dev. Discuss., https://doi.org/10.5194/gmd-2019-100, in review, 2019.

350   Sodemann, H., Aemisegger, F., Pfahl, S., Bitter, M., Corsmeier, U., Feuerle, F., Graf, P., Hankers, R., Hsiao, G., Schulz, H., Wieser, A., and Wernli, H.: The stable isotope composition of water vapour above Corsica during the HyMeX SOP1 campaign: insight into vertical mixing processes from lower-tropospheric survey flights, Atmos. Chem. Phys., 17, 6125-6151, 2017.

Stickney, T.M., Shedlov, M.W., and Thompson, D.I.: Goodrich Total Temperature Sensors, Technical Report, 5755, C, 32 pp. http://www.faam.ac.uk/index.php/faam-documents/science-instruments/47-rosemount-report-5755/file, 1994.

355   Young, I.R.: Wind generated ocean waves, Elsevier ocean engineering book series, ISBN 978-0-08-043317-2, 1st edition, 287 pp., 1999.

Figure 1. The Dornier 128-6 D-IBUF in front of a wind park on 10 August 2017. Photo: Mark Bitter, TU Braunschweig
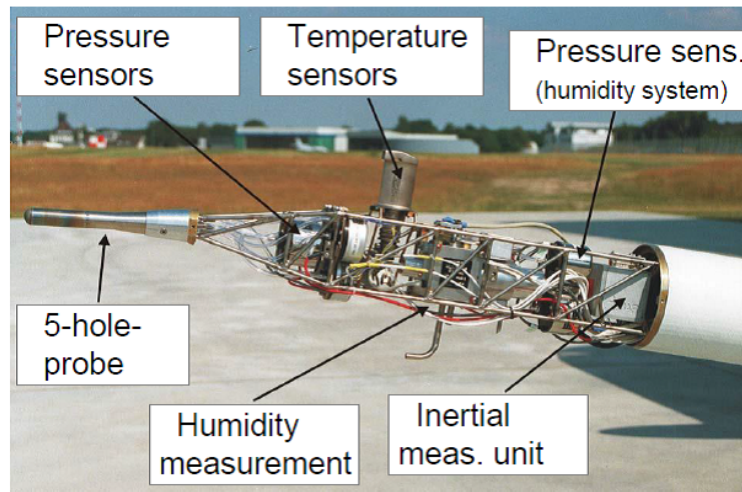
Figure 2. ~~Tracks~~ Nose boom and instrumentation of ~~all measurement flights performed during~~ the ~~WIPAFF experiment. The flight tracks are indicated in red. Each wind turbine installed until 2017 is represented by a blue dot~~research aircraft Dornier 128-6 D-IBUF. ~~The measurements were performed from the airports Wilhelmshaven~~Photo: Mark Bitter, ~~Husum and Borkum. The wind parks Godewind and Amrumbank West are indicated with a black box.~~TU Braunschweig
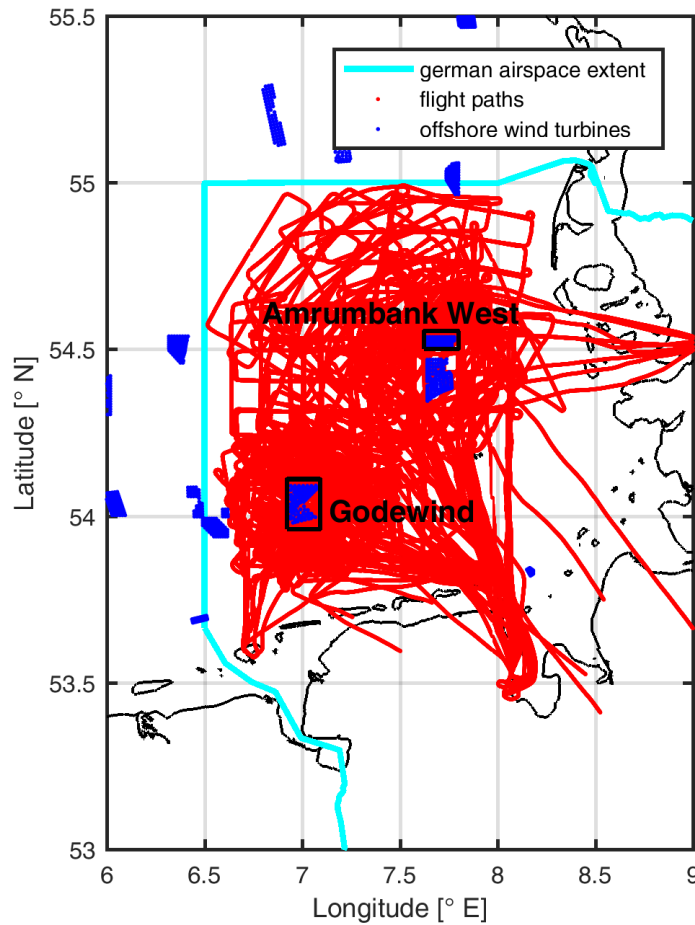
Figure 3. Tracks of all measurement flights performed during the WIPAFF experiment. The flight tracks are indicated in red. Each wind turbine installed until 2017 is represented by a blue dot. The measurements were performed from the airports Wilhelmshaven, Husum and Borkum. The wind parks Godewind and Amrumbank West are indicated with a black box. Flight tracks end when the data acquisition was shut down. The extent of the German air space is indicated by a light blue line.
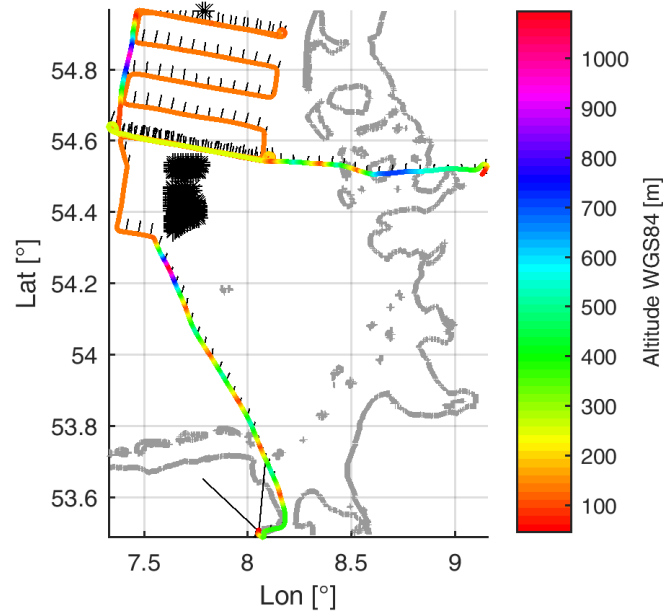
Figure 4. Example of the meander pattern to investigate the wake behind a wind park. Flight 7 was performed on 10 September 2016. It started at Wilhelmshaven airport and ended at Emden airport for refuelling. The black stars indicate individual wind turbines. The colours show the flight altitude. On the way to the wind park and back, vertical climbs and descents were performed to study atmospheric stability. The wind barbs indicate wind direction and a first idea of wind speed, which is proportional to the length of the wind barbs.
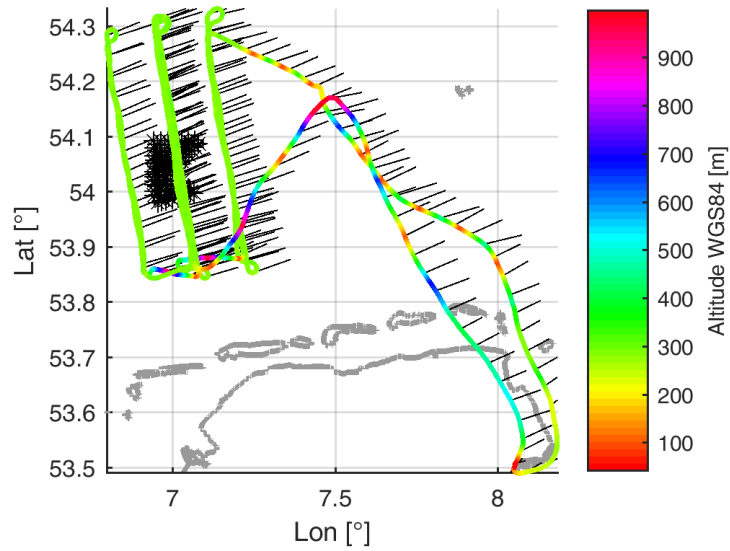
17

Figure 5. Example of the pattern above the wind park to investigate the downward mixing. Flight 39 was performed on 14 September 2017. It started and ended at Wilhelmshaven airport. The black stars indicate individual wind turbines. The colours show the flight altitude. On the way to the wind park and back, vertical climbs and descents were performed to study atmospheric stability.
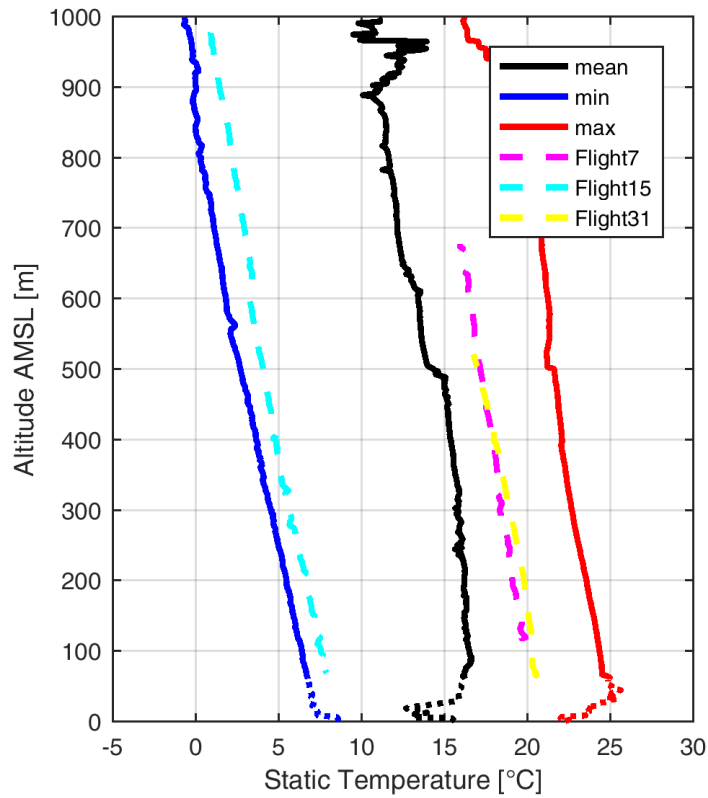
Figure 6. Average temperature profile (black) and range of temperatures (minimum blue, maximum red) encountered during the 41 WIPAFF measurement flights. Additionally, the averaged profiles of Flight 7 (magenta), Flight 15 (cyan) and Flight 31 (yellow) are included. As altitudes below 60 m altitude were only performed during take-off and landing, i.e. above land and not above the North Sea, the profiles are provided in dotted lines.

Figure 7. Average stability conditions (black) and range of stability (minimum blue, maximum red) encountered during the 41 WIPAFF measurement flights. Additionally, the averaged profiles of Flight 7 (magenta), Flight 15 (cyan) and Flight 31 (yellow) are included. As altitudes below 60 m altitude were only performed during take-off and landing, i.e. above land and not above the North Sea, the profiles are provided in dotted lines.
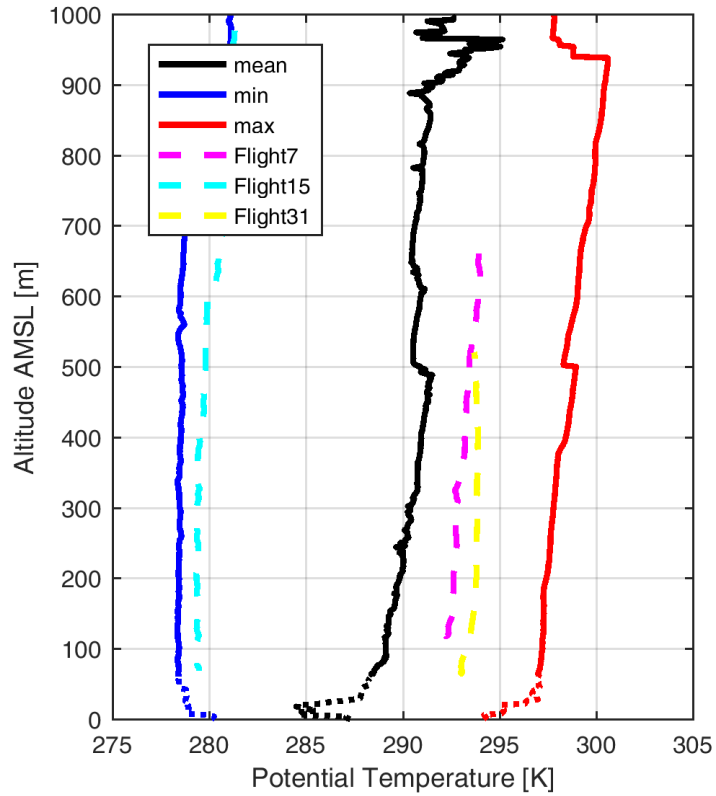
Figure 8. Average wind speed profile (black) and range of wind speed (minimum blue, maximum red) encountered during the 41 WIPAFF measurement flights. Additionally, the averaged profiles of Flight 7 (magenta), Flight 15 (cyan) and Flight 31 (yellow) are included. As altitudes below 60 m altitude were only performed during take-off and landing, i.e. above land and not above the North Sea, the profiles are provided in dotted lines.
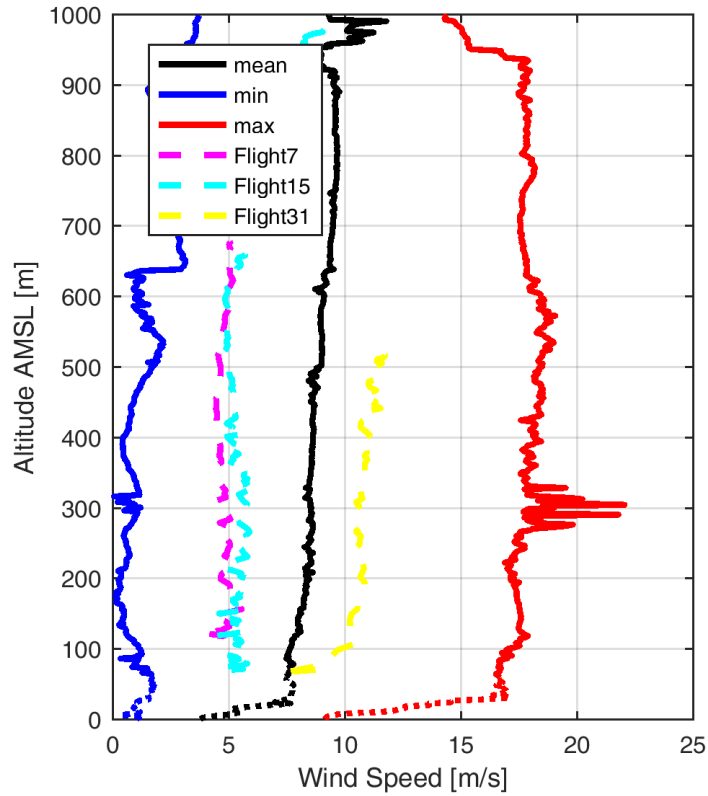
Figure 9. Average profile of water vapour mixing ratio (black) and range of mixing ratio (minimum blue, maximum red) encountered during the 41 WIPAFF measurement flights. Additionally, the averaged profiles of Flight 7 (magenta), Flight 15 (cyan) and Flight 31 (yellow) are included. As altitudes below 60 m altitude were only performed during take-off and landing, i.e. above land and not above the North Sea, the profiles are provided in dotted lines.
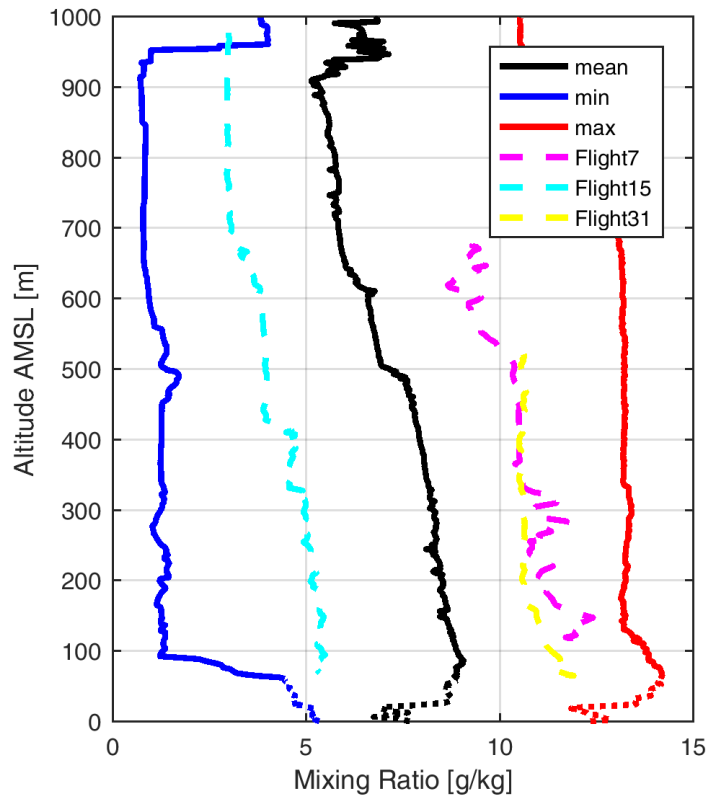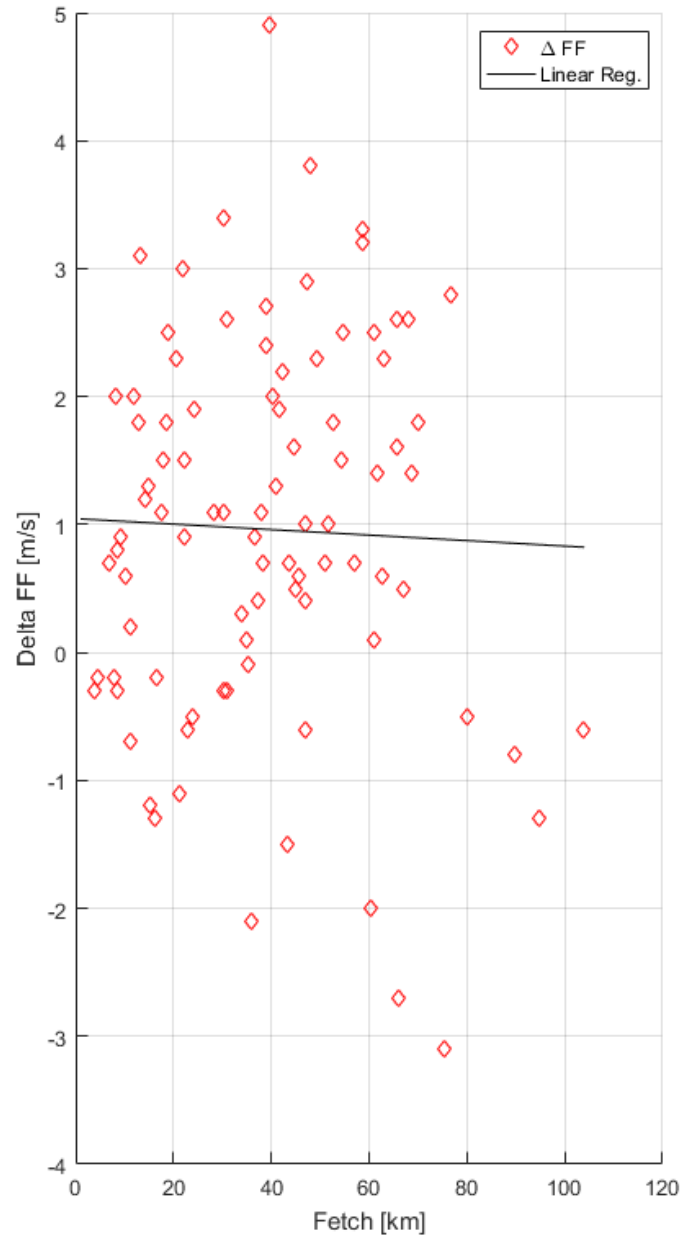
Figure 10. Changes of the wind speed at hub height (120 m) from the profile closest to the coast line to the other vertical profiles depending on fetch length. The vertical profiles of Flight 1, 3, 4, 5, 6, 7, 8, 9, 10, 13, 18, 19, 24, 30, 31, 32, 35, 36, 37, 38, 40, and 41 are included. Excluded were flights with wind direction from North or West, where no fetch length can be determined.
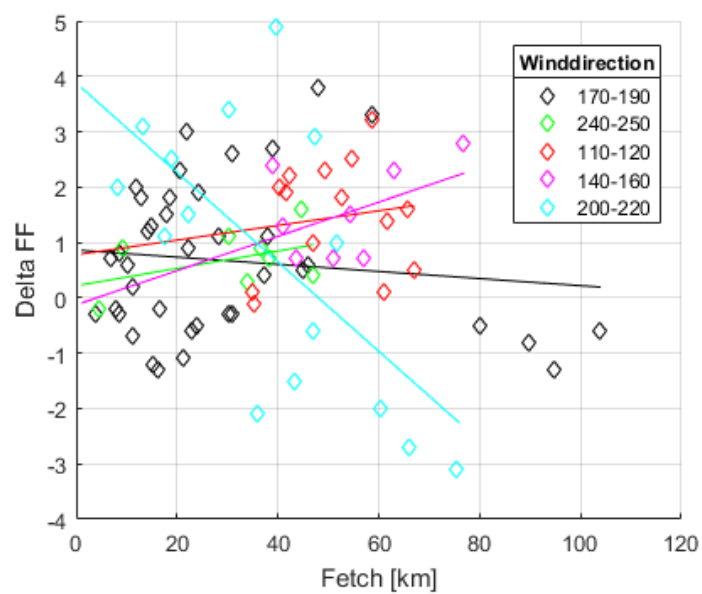
Figure 11. Changes of the wind speed at hub height as in Fig. 10. Different sectors of the wind direction are indicated in different colours.

Table 1. Overview of the WIPAFF measurement flights 1–20. The flight patterns are MEANDER(M), CROSS (C) or ABOVE (A) as indicated in Sect. 4. The wind parks are Godewind (GD) or Amrumbank West (AM). Information on cloud conditions is not always available (n.a.). Sentinel 1A and 1B satellite overpasses on the same day are indicated as well.

flight number	date	flight time [UTC] take off – landing	wind park	flight pattern	main flight altitude [m]	wind speed [m s^{-1}]	wind dir [°]	cloud conditions	satellite [UTC]
1	6 Sep 2016	12:13-15:20	AM	M	90	7	190	n.a.	-
2	7 Sep 2016	07:27-10:43	AM	M, C	90	4	210	n.a.	-
3	7 Sep 2016	12:06-13:59	AM	C	90, 120, 150	4	190	n.a.	-
4	8 Sep 2016	08:39-12:23	AM	M, C	60, 90, 120, 150	8	120	Ci	1A 17:0
5	9 Sep 2016	09:00-12:40	GD, AM	M	90, 120	6	240	n.a.	-
6	9 Sep 2016	13:42-17:10	AM	A	300	6	250	Cu	
7	10 Sep 2016	07:43-11:13	AM	M,C	60, 90, 120, 150, 200	7	190	clear sky	1A 05:4
8	10 Sep 2016	12:17-15:58	AM	M,C	60, 90, 120, 150, 200	4	190	Ci	-
9	30 Mar 2017	13:56-17:02	GD	M	120	15	240	As, Ci	1B 17:1
10	31 Mar 2017	13:36-16:59	GD	A	60, 90, 120, 200, 250	13	180	As, Ci	-
11	5 Apr 2017	13:42-16:33	GD	M,A	120, 200, 250	14	310	Sc	1A 17:1
12	6 Apr 2017	13:29-16:20	GD	M,A	120, 200, 250	10	310	Sc, As	-
13	9 Apr 2017	10:36-14:05	GD	M,C	60, 120, 200, 250	7	220	clear sky	-
14	9 Apr 2017	14:31-17:16	GD	C	60, 120, 200, 250, 350	4	200	clear sky	-
15	11 Apr 2017	09:15-13:09	GD	A	250, 300	8	280	Cu, As	-
16	11 Apr 2017	14:07-17:07	GD	M	120, 200	8	260	St, ~~rain~~ showers	1B 17:1
17	13 Apr 2017	11:23-14:40	GD	M,A	120, 250, 300	13	290	Cu	1B 05:4
18	17 May 2017	11:31-14:27	AM	C	90, 120, 150, 200, 250	8	110	Sc	-
19	17 May 2017	15:16-17:45	AM	M	220	12	120	Ac	1B 17:1
20	23 May 2017	07:53-10:41	GD	M,A	120, 250	6	250	Ci, Ac, Sc	-

Table 2. Overview of the WIPAFF measurement flights 21–41 containing the same information as in Table 1.

flight number	date	flight time [UTC] take off – landing	wind park	flight pattern	main flight altitude [m]	wind speed [m s^{-1}]	wind dir [°]	cloud conditions	satellite [UTC]
21	23 May 2017	11:18-15:10	GD	M,A	120, 250	11	310	Cu	1A 17:16
22	24 May 2017	05:40-09:33	GD	M,A	120, 240	8	300	Sc	-
23	24 May 2017	10:13-14:10	GD	A	250, 300	9	270	St	-
24	27 May 2017	08:45-11:56	AM	M	90	10	150	clear sky	-
25	27 May 2017	12:39-16:35	AM	M	90	12	140	clear sky	-
26	31 May 2017	09:04-11:45	GD	A	250	8	290	Cu	1B 05:48
27	31 May 2017	13:00-16:49	GD	A	250	9	290	Ci, Cu	-
28	1 Jun 2017	07:06-10:53	AM	A	90, 150, 210	6	300	Cu	1A 05:40
29	2 Jun 2017	06:47-10:39	AM	M	60, 90, 120, 150, 220	4	170	few Ci	-
30	8 Aug 2017	08:39-12:32	AM	M	90	10	80	St	-
31	8 Aug 2017	13:06-17:06	AM	M	90	14	80	St	-
32	9 Aug 2017	08:34-12:36	AM	A	90, 200	15	210	St, rain showers	-
33	9 Aug 2017	13:09-17:04	AM	A	90, 200	13	240	Cu, rain showers	1B 17:16
34	10 Aug 2017	10:49-14:53	AM	A	90, 200	5	340	Ac	1A 17:09
35	14 Aug 2017	10:08-14:07	AM	M	90	8	150	Ci	-
36	14 Aug 2017	14:40-18:30	AM	M	90	7	120	Ci	-
37	15 Aug 2017	07:22-11:15	GD	M	120	8	180	Sc, Ac	1A 17:17
38	17 Aug 2017	06:06-10:09	AM	M	90	11	160	St	1A 05:49
39	14 Oct 2017	12:59-16:40	GD	A	250	15	260	St	1A 17:17
40	15 Oct 2017	07:06-11:08	GD	A	250	14	200	clear sky	-
41	15 Oct 2017	11:48-15:51	GD	M	120	13	190	clear sky	-